Central European Journal of Energetic Materials
ISSN 1733-7178; e-ISSN 2353-1843

Cent. Eur. J. Energ. Mater. 2021, *18*(1): 5-24; DOI 10.22211/cejem/134652
Article is available in PDF-format, in colour, at:
http://www.wydawnictwa.ipo.waw.pl/cejem/Vol-18-Number1-2021/CEJEM_01100.pdf

Research paper

Theoretical Simulations on Physicochemical Performance of Novel High-energy BHDBT-based Propellants

Ke Wang, Hai-tao Huang, Hui-xiang Xu, Huan Li, Jun-qiang Li, Xue-zhong Fan, Wei-qiang Pang*

Xi'an Modern Chemistry Research Institute, Xi'an 710065, China
* *E-mail:* 769711103@qq.com

Abstract: Based on Energy Calculation Star program and molecular dynamic method, three designed 2,3-bis(hydroxymethyl)-2,3-dinitro-1,4-butanediol tetranitrate-based (BHDBT) propellants are firstly reported and their physicochemical performance are investigated. Results suggest that compared with HMX-based and CL-20-based propellants, the specific impulses of all BHDBT-based propellants surpass or approximate 280 s, which indicates the latter have the potential to be high-energy propellants. The diffusion coefficient of plasticizers in BHDBT-based propellant decrease as the temperature reduces, and reduce in the order: Bu-NENA > TMETN > BTTN. The densities of all BHDBT-based propellants surpass or approximate 1.7 g/cm^3. The comparison of elastic constants, Poisson's ratios and K/G values indicates that the mechanical properties of three BHDBT-based propellants increase in the order (by plasticizer): Bu-NENA < TMETN < BTTN. The bond length analysis of C–NO_2 and O–NO_2 bond in BHDBT suggests that the former is the trigger bond in the BHDBT-based propellants, and the safety of BHDBT-based propellants and BHDBT crystal decreases in the order: GAP/BTTN/Al/BHDBT > GAP/Bu-NENA/Al/BHDBT ≈ GAP/TMETN/Al/BHDBT > BHDBT. In conclusion, GAP/BTTN/Al/BHDBT propellant has the potential to be a novel high-energy propellant.

Keywords: molecular dynamic, BHDBT, migration, mechanical properties, safety

1 Introduction

Solid propellants are drawing more and more attention of scientists serving as the sources of energy for ultra range rockets, and the level of their energy determines the range and load of rockets [1, 2]. Therefore, high-energy propellants which can realize remote, high-precision and more powerful missions have been an important developing orientation. Therein, adding novel high-energy density materials (HEDMs) or enhancing the solid content in the formulation of propellants are effective ways to improve the energy of propellants, which are worth constantly exploring, improving and innovating [3-5]. Due to high density and heats of formation (HOF), large numbers of nitric acid ester, furazan-based derivatives and nitrogen-rich heterocycles have strongly attracted the interest of experts [6-8]. Therein, 2,3-bis(hydroxymethyl)-2,3-dinitro-1,4-butanediol tetranitrate (BHDBT, as shown in Figure 1) [9, 10], whose level of energy approximates HMX, and the decomposition temperature exceeds 150 ºC, has the potential to be a novel oxidant in high-energy propellants. Sizov *et al.* [11] studied properties of BHDBT, and results showed that BHDBT might be used in catalyzed double-base propellants as a partial substitute for nitroglycerin (NG) and increase the ballistic properties of propellants. Reese *et al.* [12] found that the ignition sensitivity and physical properties of BHDBT-based composite propellants are comparable to those of ammonium perchlorate (AP)-based formulations and may offer a promising perchlorate-free alternative to existing AP-based formulations. Bin *et al.* [13] investigated the compatibilities of BHDBT with hydroxy-terminated-polybutadiene (HTPB) propellant components by differential scanning calorimetry (DSC), and their results suggested that the mixed system of BHDBT with cyclotetramethylene tetranitramine (HMX), cyclotrimethylene trinitramine (RDX) and Al powder was compatible, with AP was slightly sensitive, and HTPB and TDI was incompatible. However, BHDBT is mainly used as a substituent or additive of propellant systems in the current study, and there are few comprehensive studies on BHDBT serving as a main oxidant in solid propellants.

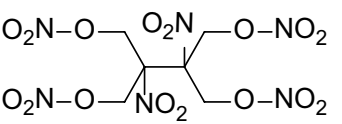

Figure 1. The framework of BHDBT

Theoretical simulation can help fully understand the relationships between performance and composition of systems. As a result, much better

and more efficient experimental preparation and application can be performed based on theoretical simulation. Therein, the molecular dynamic (MD) method is an effective way to predict the dynamic, thermal, mechanical and diffusion behavior of composites, which is in reasonably good agreement with experimental measurements [14]. Zhu *et al.* [15] investigated the safety performance (sensitivity), thermal expansion and mechanical properties of solid propellants by MD simulation. Ma *et al.* [16] studied the interfacial, mechanical properties of 5,5'-bis(tetrazole)-1,1'-diolate-based (TKX-50) PBX and the desensitizing mechanisms of binder for TKX-50. Therefore, the MD method is an efficient and accurate tool to study the performance of multi-component systems.

In this work, the physicochemical performances of three BHDBT-based propellants are predicted. Firstly, their related energy parameters are calculated by Energy Calculated Star (ECS) program; secondly, the migration of plasticizers in BHDBT-based propellants and their mechanical properties are calculated by the MD method; and finally, the safety of the three propellants is estimated and compared with BHDBT. In conclusion, it is hoped that this work can help guide the BHDBT-based propellants preparation and application.

2 Calculated Details

2.1 Energy calculations

The ECS [17] program was applied to predict parts of the physicochemical performance of propellants based on BHDBT, and it was found that the theoretically specific impulses of propellants surpass or approximate 280 s when the proportion of components reaching constant values. The mass ratio of formulations is listed in Table 1. The calculated conditions are as follow: the original temperature of propellant is 298 K; the pressure of thrust chamber is 7 MPa; the outlet pressure of nozzle is 0.1 MPa.

Table 1. The mass ratio of each component in formulations

Formulation	Mass ratio [%]					
	GAP	Bu-NENA	BTTN	TMETN	Al	BHDBT
1	12	8	–	–	13	67
2		–	8	–		
3		–	–	8		

2.2 Model building

Based on the formulations of the high-energy propellants in Table 1, their correspondingly amorphous cells were constructed using Amorphous Cell Module in Material Studio 8.0 [18], and the number of molecules of corresponding components are listed in Table 2, therein, the mole mass of GAP is 3700 g/mol. All cells were optimized using COMPASS force field (Forcite Module), which is effective to investigate the properties of the condensed phase [19, 20]. Van der Waals force and Electrostatic interaction were calculated using the atom-based and Ewald methods [21, 22], respectively.

Table 2. The number of molecule in each formulation

Formulation	The number of molecule					
	GAP	Bu-NENA	BTTN	TMETN	Al	BHDBT
1	3	30	–	–	494	117
2		–	26	–	489	116
3		–	–	25	497	118

2.3 Molecular dynamic simulation

The structural relaxation of optimized structures were performed under 50 ps constant particle number, pressure, and temperature (NPT) ensemble, 50 ps constant particle number, volume, and temperature (NVT) ensemble, and annealing simulation (temperature from 300 to 500 K).

The relaxed structures were used to perform the MD simulation. The total calculated time was 1000 ps, and the time step was 1 fs. The given temperature and pressure were 298 K and 100 kPa, respectively. The Anderson and Berendsen methods were used to control temperature and pressure, respectively [23, 24]. The initial velocity was sampled by the Maxwell distribution, and velocity Verlet arithmetic was utilized [25]. The van der Waals force and Electrostatic interaction were calculated by the atom-based and Ewald methods, respectively [21, 22]. The final 300 ps was applied to predict mechanical properties. And the finally balanced structures of three systems of BHDBT-based propellants are presented in Figure 2.

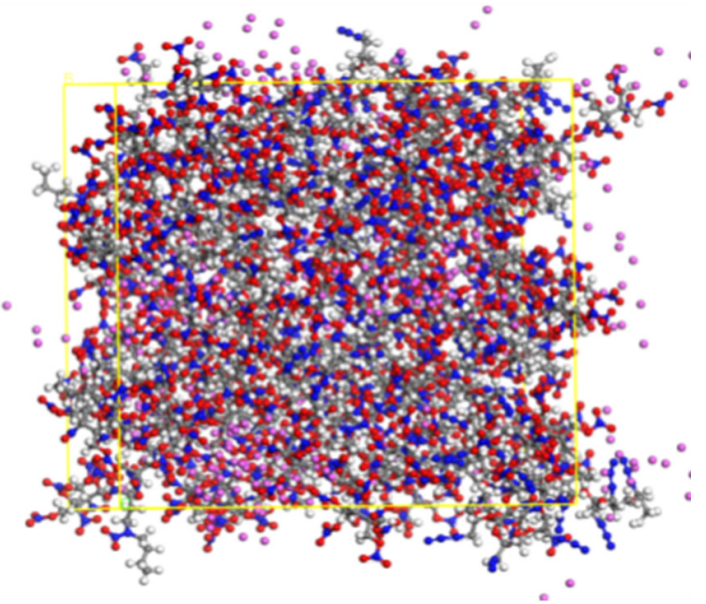

(a) GAP/Bu-NENA/Al/BHDBT

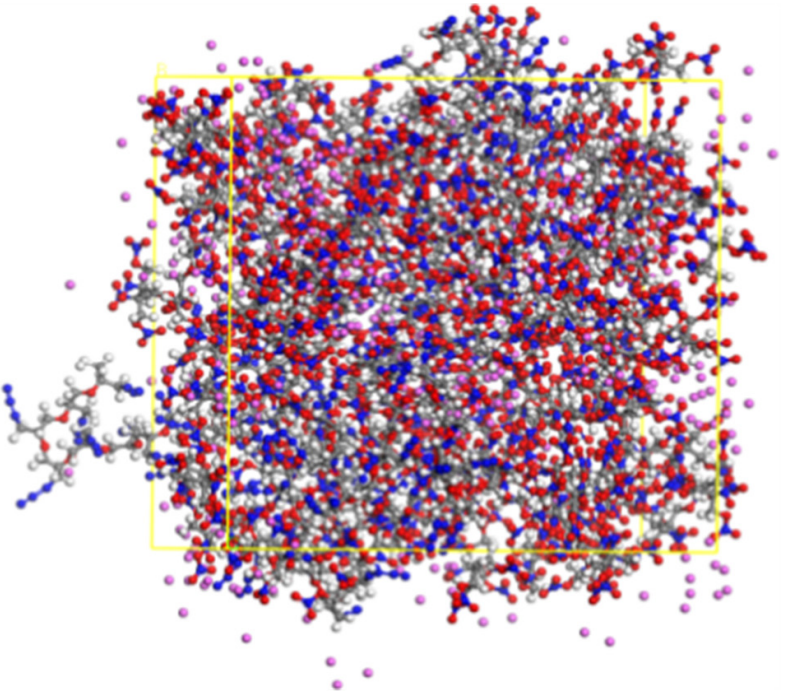

(b) GAP/BTTN/Al/BHDBT

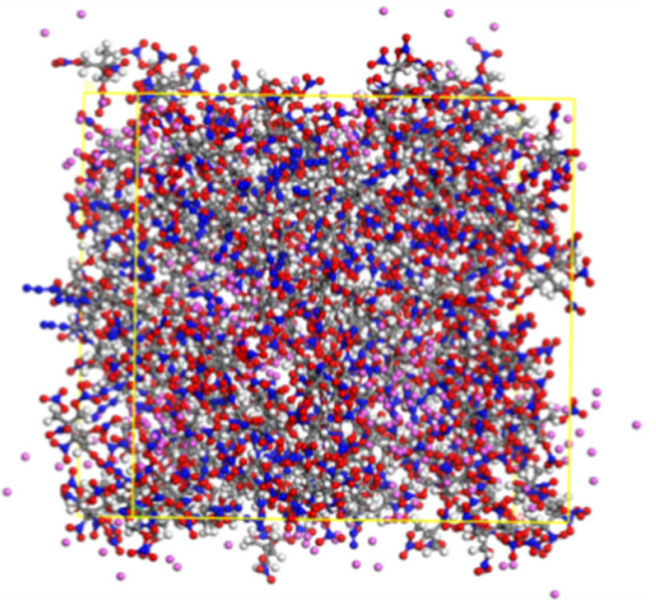

(c)

Figure 2. The balanced structures of high-energy propellants containing BHDBT at 298 K: (a) GAP/Bu-NENA/Al/BHDBT, (b) GAP/BTTN/Al/BHDBT and (c) GAP/TMETN/Al/BHDBT

2.4 Calculation of migration

Based on balanced structures, three systems of high-energy propellants were performed using 500 ps MD calculation (NVT ensemble), and the computing method and parameters were as above. The temperature was successively set to 323, 293, 273 and 233 K. The ultimate consequences were used to analyze the mean square displacement (MSD) of different plasticizers.

2.5 Calculation of mechanical properties

The last 300 ps of equilibrium trajectory documents at 298 K were applied to calculate the mechanical properties of three BHDBT-based propellants. The elastic constants were obtained by performing the mechanical analysis in MS, and the related mechanical parameters could be evaluated. The generalized Hooke's law is written as Equation 1:

$$\sigma_i = C_{ij}\varepsilon_j \tag{1}$$

where σ_i is the stress tensor (GPa), C_{ij} is the 6×6 stiffness matrix of elastic

constants, and ε_j is the strain tensor (GPa). Meanwhile, the stiffness matrix of the stress-strain behavior of isotropic material can be described by the Lamé coefficients (λ and μ), as shown in Equation 2 [26]:

$$\begin{matrix} \lambda+2\mu & \lambda & \lambda & 0 & 0 & 0 \\ \lambda & \lambda+2\mu & \lambda & 0 & 0 & 0 \\ \lambda & \lambda & \lambda+2\mu & 0 & 0 & 0 \\ 0 & 0 & 0 & \mu & 0 & 0 \\ 0 & 0 & 0 & 0 & \mu & 0 \\ 0 & 0 & 0 & 0 & 0 & \mu \end{matrix} \tag{2}$$

In the end, the elastic modulus of isotropic material can be predicted by the Lamé coefficients as follows [27-29]:

$$E = \mu \frac{3\lambda + 2\mu}{\lambda + \mu} \tag{3}$$

$$K = \lambda + \frac{2}{3}\mu \tag{4}$$

$$G = \mu \tag{5}$$

$$\gamma = \frac{\lambda}{2(\mu+\lambda)} \tag{6}$$

where E is Young's modulus (GPa), K is bulk modulus (GPa), G is shear modulus (GPa), and γ is Poisson's ratio.

3 Results and Discussion

3.1 Energy characteristics

The physical parameters of the components are listed in Table 3. Afterwards, the energy characteristics of the propellants are predicted using the ECS program based on the heats of formation (ΔH_f) and the chemical formulas of the components. Therein, the specific impulse (I_{sp}) is used to compare

the performances of solid rocket propellants, its value being of utmost significance for the propellant, as it determines whether the propellant meets the ballistic requirements. Meanwhile, the maximum I_{sp} values of HMX-based, CL-20-based and BHDBT-based propellants based on calculations of different mass ratios are shown in Table 4. Therein, the mass ratio of the binder system (binder *vs.* plasticizer) remains 12:8 in the formulation of propellants.

Table 3. Physical parameters of the components

Components	ρ [g/cm^3]	ΔH_f [kJ/mol]
GAP	1.30	141.003
Bu-NENA	1.21	459.413
BTTN	1.52	–406.960
TMETN	1.46	–425.091
BHDBT	1.82	–371.00
Al	2.70	0
HMX	1.91	75.016
CL-20	1.98	415.5

Table 4. The formulation of HMX-based and CL-20-based propellants

System	GAP/Bu-NENA	GAP/BTTN	GAP/TMETN
HMX:Al	68:12	66:14	
CL-20:Al			
BHDBT:Al	63:17		

The results of energy characteristics are presented in Table 5, meanwhile, BHDBT-based propellants possessing same formulation as HMX-based and CL-20-based propellants are also listed as reference value. It is easily seen that the specific impulse (I_{sp}), characteristic velocity (C^*), combustion temperature (T_c) and oxygen balance (OB) of BHDBT-based propellants are larger than those of HMX-based and CL-20-based propellants even if the formulation of the former are same as those of the latter. However, the average relative molecular mass of combustion gas ($\overline{M}$) of the former are lower than those of the latter. In the end, the I_{sp} of propellants containing BHDBT overpass or approximate 280 s, which exhibits high energy compared with HMX-based (265-271 s) and CL-20-based (266-269 s) propellants.

Table 5. The energy characteristics of BHDBT-based propellants, HMX-based propellants and CL-20-based propellants

Formulation		I_{sp} [s]	C^* [m/s]	T_c [K]	$\overline{M}$ [mol/kJ]	*OB*
BHDBT	Bu-NENA	280.76	881.1	2384.87	36.66	0.533
	BTTN	279.70	881.5	2603.39	34.42	0.593
	TMETN	279.86	881.3	2558.53	34.83	0.580
BHDBT (reference values)	Bu-NENA	280.03	880.7	2326.16	37.24	0.581
	BTTN	279.54	880.4	2509.95	34.69	0.624
	TMETN	279.66	879.6	2462.52	35.11	0.611
HMX	Bu-NENA	265.84	742.3	1611.43	43.61	0.416
	BTTN	271.15	773.9	1884.96	40.81	0.446
	TMETN	270.21	853.4	1847.03	41.22	0.443
CL-20	Bu-NENA	266.22	836.4	1863.67	39.27	0.459
	BTTN	269.64	864.9	2193.39	36.70	0.501
	TMETN	269.03	863.0	2147.60	37.15	0.489

The relationship between I_{sp}, T_c and $\overline{M}$ is presented in Equation 7 [30]:

$$I_{sp} \propto \left(T_c \overline{M}\right)^{1/2} \tag{7}$$

It is obvious that I_{sp} is directly proportional to T_c and $\overline{M}$. Despite the $\overline{M}$ of HMX-based and CL-20-based propellants surpassing that of BHDBT-based propellants, the T_c values of the former are substantially lower than those of the latter, which results from the higher *OB* because BHDBT possesses much more oxygen. Therefore, propellants containing BHDBT exhibit higher I_{sp}. Meanwhile, propellants containing BHDBT possess faster C^* owning to their higher T_c.

3.2 Migration

The migration of plasticizer in propellants is dangerous for their application, as it may result in the inhomogeneous distribution of components in propellant grains. Ultimately, the inhomogeneous distribution may change the ballistic properties and even result in unexpected explosion. The migration of plasticizer is described by its diffusion coefficient (*D*), which depends on the MSD and time (*t*) of MD simulation. *D* is described in Equation 8, which is based on Einstein's equation [31, 32]:

$$D = \lim_{t\to\infty} \frac{\left\langle \left| r(t) - r(0) \right|^2 \right\rangle}{6t} \tag{8}$$

where $r(t)$ is coordinate of plasticizer at time t, and $r(0)$ is the original coordinate.

The relationship of MSD is calculated by Equation 9 [33]:

$$\text{MSD} = s(t) = \left\langle \left| r(t) - r(0) \right|^2 \right\rangle \tag{9}$$

The D is ultimately estimated by Equations 8 and 9 [33]:

$$D = s(t) / 6t = m / 6 \tag{10}$$

where m is the slope of the MSD-t curve.

The MSD of plasticizers (Bu-NENA, BTTN and TMETN) were predicted using MD calculation. The MSD-t curves of BHDBT-based propellants and their linear fitting curves at different temperatures are presented in Figure 3. It is obvious that all curves are almost linear (except the MSD-t curves of Bu-NENA at 323 K). The slopes (m) of the linear fitting curves and the diffusion coefficients (D) are presented in Table 6.

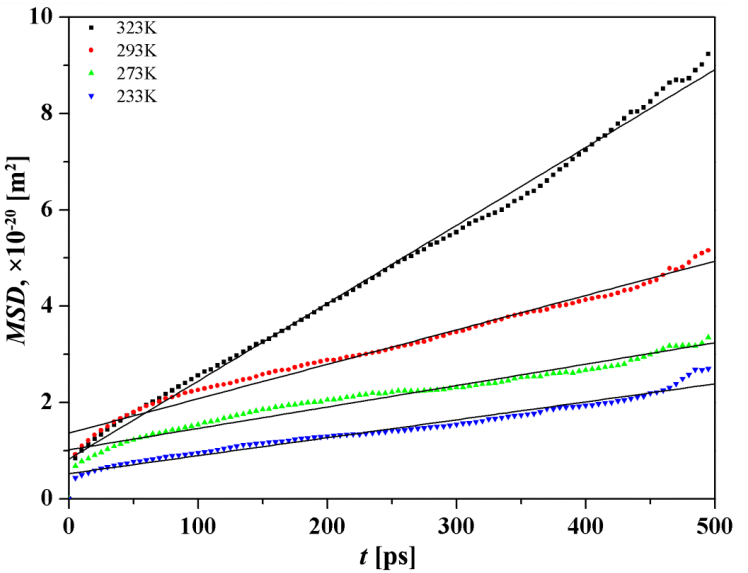

(a)

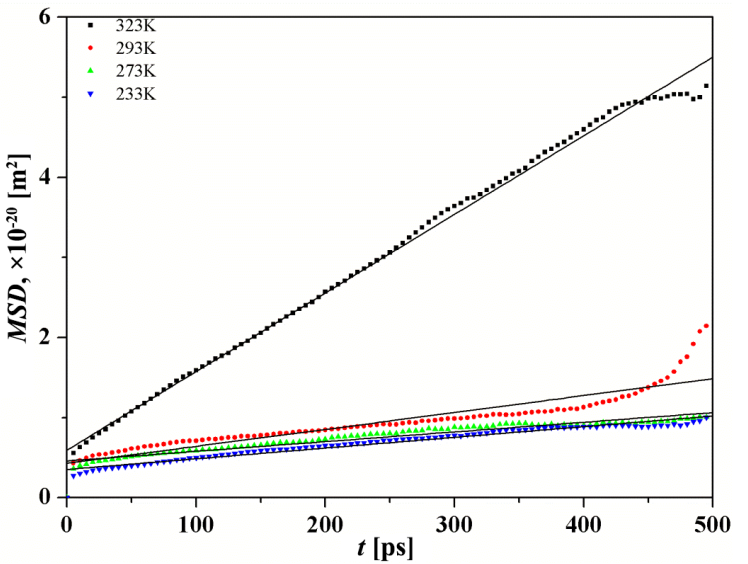

(b)

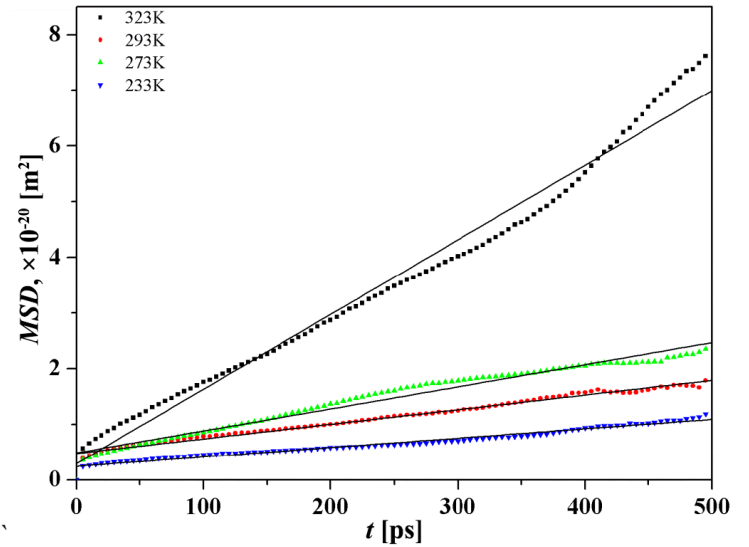

(c)

Figure 3. The MSD-t curves of high-energy propellants containing BHDBT in different temperatures for: (a) Bu-NENA, (b) BTTN and (c) TMETN

Table 6. The diffusion coefficients of high-energy propellants containing BHDBT at different temperatures

T [K]	Bu-NENA		BTTN		TMETN	
	m	*D*	*m*	*D*	*m*	*D*
	$\times 10^{11}$ [m^2/s]		$\times 10^{11}$ [m^2/s]		$\times 10^{11}$ [m^2/s]	
323	16.17	2.70	9.82	1.64	13.41	2.24
293	7.15	1.19	2.12	0.35	2.63	0.44
273	4.44	0.74	1.21	0.20	3.96	0.66
233	3.72	0.62	1.33	0.22	1.69	0.28

It is easy to see that the *D* values of all plasticizers decrease as the temperature is reduced. The Bu-NENA and BTTN possess the highest and lowest *D* values at every temperature, which indicates the former migrates the most easily in BHDBT-based propellants. And with increasing temperature, the migration of plasticizers exhibits a decreasing trend. When the temperature is reduced to 293 K, the values of *D* of the plasticizers all substantially decrease. However, the value of *D* for Bu-NENA is still significantly higher than the others as is also the case at 323 K. At 273 K, the value of *D* for TMETN exhibits a small increase which may be due to the glass transition of the system. Meanwhile, the migration of BTTN and Bu-NENA still decreases by a small amount. For all systems at a temperature of 233 K, the *D* values of Bu-NENA and TMETN all reduce, but that of BTTN shows a small increase. In conclusion, the migration of three plasticizers in BHDBT-based propellants decreases in the order: Bu-NENA > TMETN > BTTN.

3.3 Mechanical properties

The mechanical properties are important parameters for propellants and are related to their preparation, process and application. The elastic constants and related parameters of the BHDBT-based propellants are listed in Table 7.

Table 7. The elastic constants and related parameters of BHDBT-based high-energy propellants

System	GAP/Bu-NENA/ Al/BHDBT	GAP/BTTN/ Al/BHDBT	GAP/TMETN/ Al/BHDBT
λ	3.5599	1.8915	1.6565
μ	2.0547	1.5350	1.8222
C_{11}	7.9886	5.3382	7.0894
C_{22}	8.3879	4.3326	3.5067
C_{33}	6.6314	5.2136	5.3063
C_{44}	2.1567	2.1228	1.9968
C_{55}	2.3903	0.6192	1.5766
C_{66}	1.6172	1.8631	1.8931
C_{12}	3.7091	2.8278	2.5984
C_{13}	3.5070	2.7959	3.5113
E [GPa]	5.412	3.945	4.512
K [GPa]	4.930	3.078	2.873
G [GPa]	2.055	1.535	1.822
γ	0.317	0.286	0.238
K/G	2.399	2.005	1.577
ρ [g/cm^3]	1.697	1.752	1.741

The densities of the three systems are 1.697, 1.752 and 1.741 g/cm^3 when the plasticizers are respectively Bu-NENA, BTTN and TMETN, which are all high values. All diagonal elements (C_{ii}) and off-diagonal elements (C_{ij}) gradually decrease when the plasticizer changes from Bu-NENA to TMETN, which indicates that TMETN may better reduce the anisotropy of the system. The elastic constants are predicted from the Lamé coefficients. It is easy to see that the Young's modulus (E), the bulk modulus (K), and the shear modulus (G) of the GAP/Bu-NENA/Al/BHDBT system all have the highest values, while those of the GAP/BTTN/Al/BHDBT system are the lowest (except for K). Otherwise, the elastic constants of the GAP/TMETN/Al/BHDBT system are close to the latter. It suggests that BTTN and TMETN can better attenuate the stiffness, improve the elasticity and decrease the brittleness of BHDBT-based propellants. Otherwise, the larger value of the Cauchy pressure (K/G) is, the better is the ductility of the system [26]. It is obvious that the ductility of the system is best when the plasticizer is Bu-NENA, and worst when the plasticizer is TMETN. The Poisson's ratios (γ) of the three systems are all within the range 0.2-0.4, which indicates that all systems exhibit good plasticity and will be easy to process. In conclusion, based on the analysis

of elasticity and ductility, the mechanical properties of the three system decreases in the order:

GAP/BTTN/Al/BHDBT > GAP/TMETN/Al/BHDBT > GAP/Bu-NENA/Al/BHDBT.

3.4 Safety

Safety is a crucial parameter for solid rocket propellants, and determines the development of modern weapons [15]. The first stage in the decomposition of BHDBT is the cleavage of NO_2 groups at 154 ºC. Meanwhile, the potentially original trigger bond lengths of the C–NO_2 and O–NO_2 bonds in BHDBT are respectively 1.550 and 1.406-1.427 Å, the former bond being the more unstable [10, 11]. Therefore, the potential trigger bonds (C–NO_2 and O–NO_2) of BHDBT were analyzed as they may be the most likely components to initiate detonation. The bond lengths of the trigger bonds of BHDBT in the three high-energy propellants were calculated. Otherwise, the original crystal cell of BHDBT (as shown in Figure 4) was selected to compare the bond lengths of the trigger bonds for three high-energy propellants. The calculation method was as follows: the 3×1×3 supercell of BHDBT was constructed based on its original cell, and then the MD-NPT simulation was performed (the method being the same as in section 2.3 above) after optimization of supercell. The bond lengths of the trigger bonds of the BHDBT supercell were predicted and the results are presented in Table 8.

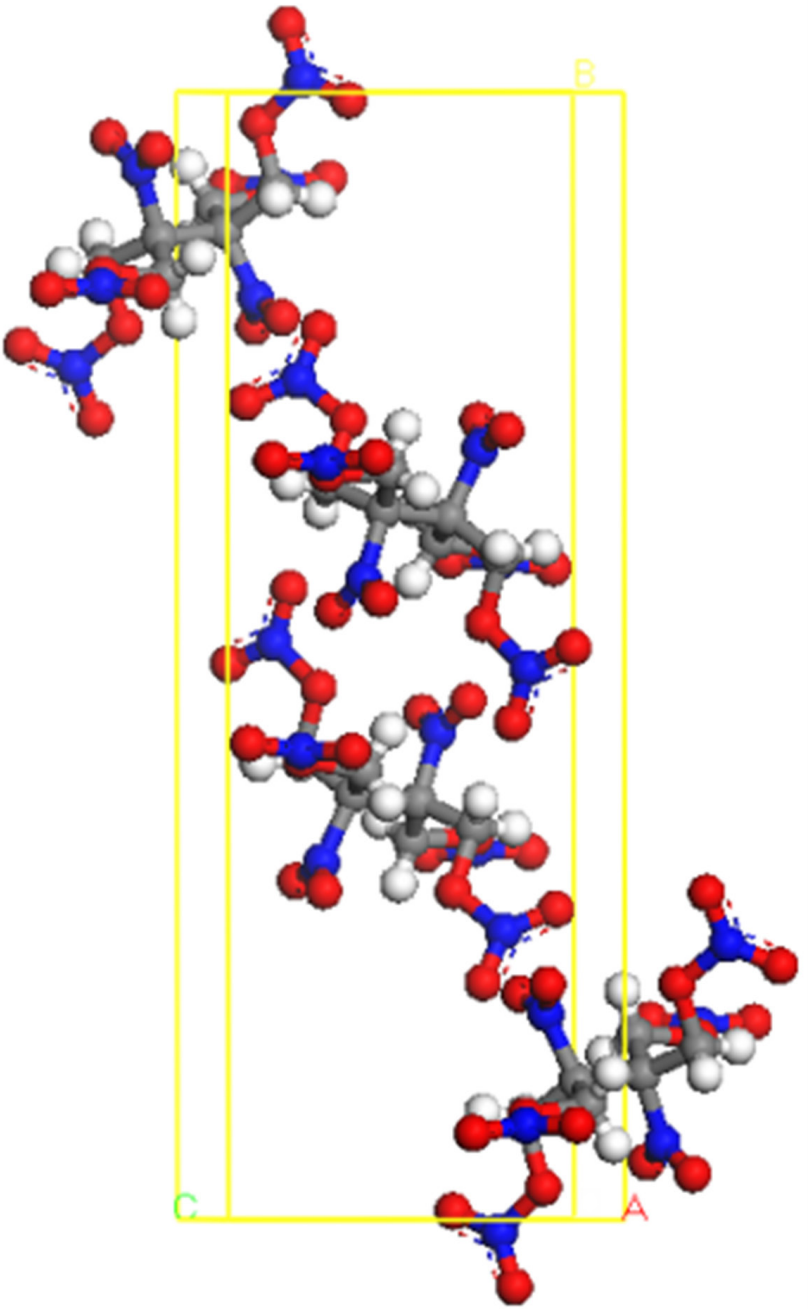

Figure 4. The crystal structure of BHDBT

Table 8. The average bond lengths and the maximum bond lengths of $C–NO_2$ and $O–NO_2$ of BHDBT in BHDBT-based propellants and BHDBT supercell

System	$C–NO_2$		$O–NO_2$	
	λ_{ave} [Å]	λ_{max} [Å]	λ_{ave} [Å]	λ_{max} [Å]
BHDBT	1.498	1.620	1.478	1.525
GAP/Bu-NENA/Al/BHDBT	1.495	1.580	1.442	1.475
GAP/BTTN/Al/BHDBT	1.494	1.540	1.444	1.475
GAP/TMETN/Al/BHDBT	1.496	1.580	1.442	1.475

The distribution curves of the bond lengths of the trigger bonds are presented in Figures 5 and 6. Meanwhile, the bond lengths of average (λ_{ave}) and largest (λ_{max}) trigger bonds are listed in Table 8. It is easy to see that the lengths of the $C–NO_2$ bonds in every system are larger than those of the $O–NO_2$ bonds, indicating that the $C–NO_2$ bond is more unstable and easier to rupture under an external stimulus. This is consistent with the reference. Compared with the BHDBT supercell, the λ_{ave} and λ_{max} of the $C–NO_2$ bond and $O–NO_2$ bonds are all shorter no matter what the plasticizer is. This indicates that the propellant systems improve the safety of BHDBT, which may result from van der Waals forces between BHDBT and other components in the propellants. Otherwise, when the plasticizer is BTTN, the $C–NO_2$ bond lengths (λ_{ave} = 1.494 Å, λ_{max} = 1.540 Å) are all shorter than those in other propellants. This indicates that the GAP/BTTN/Al/BHDBT propellant possesses the best safety, which is consistent with the mechanical properties all resulting from the best plasticizing effect of BTTN. In addition, when the plasticizer is Bu-NENA or TMETN, the lengths of the $C–NO_2$ and $O–NO_2$ bonds are almost equal. In conclusion, the safety of three BHDBT-based high-energy propellants decreases in the order:

GAP/BTTN/Al/BHDBT > GAP/TMETN/Al/BHDBT ≈ GAP/Bu-NENA/Al/BHDBT.

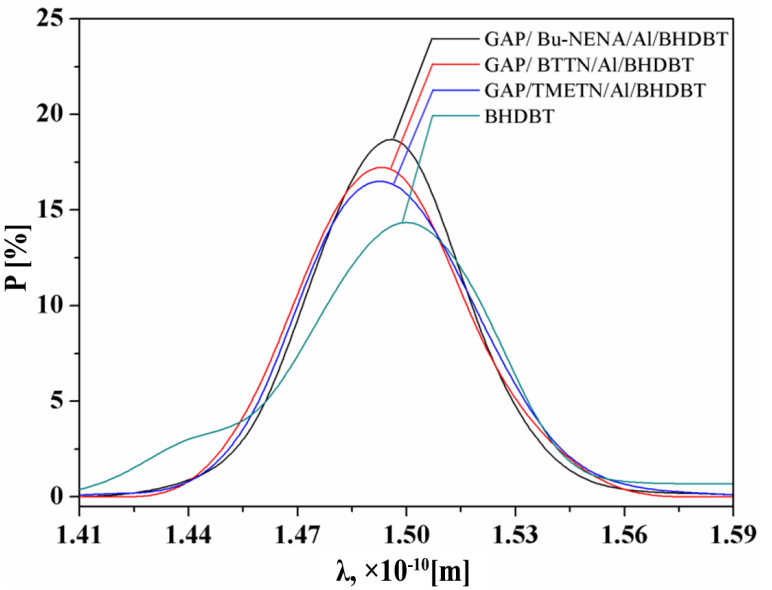

Figure 5. The C–NO_2 bond lengths (λ) *versus* the percentages (P) of BHDBT in BHDBT-based propellants and BHDBT supercell

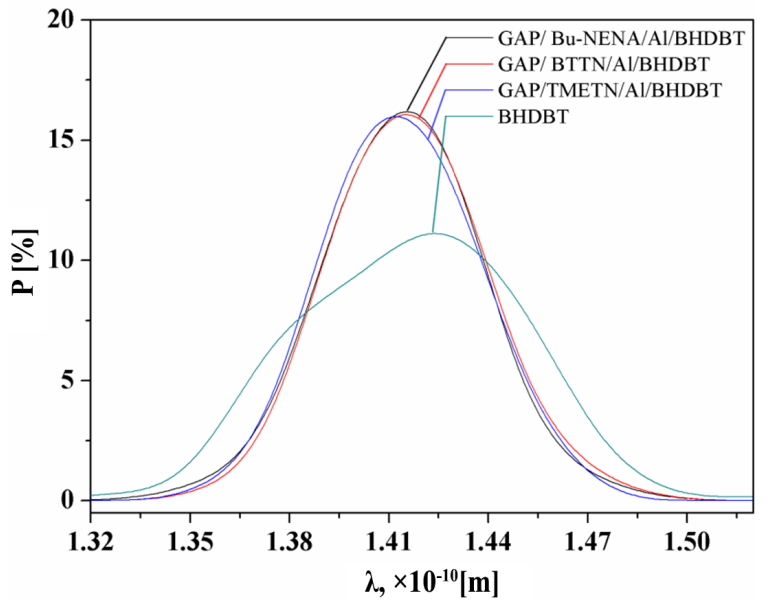

Figure 6. The N–NO_2 bond lengths (λ) *versus* the percentages (P) of BHDBT in BHDBT-based propellants and BHDBT supercell

4 Conclusions

Three novel BHDBT-based propellants have been designed, and their specific impulse, migration of plasticizers, mechanical properties and safety are predicted based on the ECS program and MD simulation. The main results are as follows:

- The I_{sp} values of three BHDBT-based propellants all surpass or approximate 280 s, which are superior those of HMX-based and CL-20-based propellants, when their mass ratio of binder systems remain constant. And it is impressive that they have the potential to be high-energy propellants.
- All the diffusion coefficients of plasticizers decrease with a reduction in temperature. And by comparing the diffusion coefficients, the migration of three plasticizers in BHDBT-based propellants decreases in the order:

  Bu-NENA > TMETN > BTTN.
- The densities of all BHDBT-based propellants surpass or approximate 1.7 g/cm^3. The mechanical properties of three propellants decrease in the order:

  GAP/BTTN/Al/BHDBT > GAP/TEMTN/Al/BHDBT > GAP/Bu-NENA/Al/BHDBT,

  which indicates that GAP/BTTN/Al/BHDBT system is the easiest to process.
- The C–NO_2 bond in BHDBT is the trigger bond in the BHDBT-based propellants, and it becomes difficult to rupture compared with BHDBT crystal when applied in our propellant formulations. In the end, the safety of BHDBT-based propellants decreases in the order:

  GAP/BTTN/ Al/BHDBT > GAP/TMETN/Al/BHDBT ≈ GAP/Bu-NENA/Al/BHDBT.

References

[1] Yoshimura, T.; Esumi, K. Synthesis and Surface Properties of Anionic Gemini Surfactants with Amide Groups. *J. Colloid Interface Sci.* **2004**, *276*(1): 231-238.
[2] Lempert, D.; Nechiporenko, G.; Manelis, G. Energetic Performances of Solid Composite Propellants. *Cent. Eur. J. Energ. Mater.* **2011**, *8*(1): 25-38.
[3] Kanti Sikder, A.; Reddy, S. Review on Energetic Thermoplastic Elastomers (ETPEs) for Military Science. *Propellants Explos. Pyrotech.* **2013**, *38*(1): 14-28.
[4] Pei, Q.; Zhao, F.-Q.; Gao, H.-X.; Xu, S.-Y.; Hao, H.-X.; Yao, E.-G.; Zhou, Z.-M. Research on Application of Energetic Triazole Ionic Salts in Solid Propellant. (in Chinese) *Acta Armamentarii* **2014**, *35*(92): 1387-139.

[5] Sivabalan, R.; Talawar, M.; Senthilkumar, N.; Kavitha, B.; Asthana, S.N. Studies on Azotetrazolate based High Nitrogen Content High Energy Materials Potential Additives for Rocket Propellants. *J. Therm. Anal. Calorim.* **2004**, *78*(3): 781-792.
[6] Shao, H.-s.; Ling, Yi-f., L.; Hou, T.-j.; Ruan, H.-w.; Wang, Ch.-j.; Luo, J. Synthesis and Characterization of 9-Nitro-9-azabicyclo [3.3.1]nonane-2,6-diyl Dinitrate. (in Chinese) *Chin. J. Explos. Propellants* **2016**, *39*(2): 64-67.
[7] Stepanov, A.I.; Dashko, D.V.; Astrat'ev, A.A. 3,4-Bis(4'-nitrofurazan-3'-yl)furoxan: a Melt Cast Powerful Explosive and a Valuable Building Block in 1,2,5-Oxadiazole Chemistry. *Cent. Eur. J. Energ. Mater.* **2012**, *9*(4): 329-342.
[8] Fischer, N.; Fischer, D.; Klapötke, T.M.; Piercey, D.G.; Stierstorfer J. Pushing the Limits of Energetic Materials – the Synthesis and Characterization of Dihydroxylammonium 5,5'-Bistetrazole-1,1'-diolate. *J. Mater. Chem.* **2012**, *22*(38): 20418-20422.
[9] Chavez, D.E.; Hiskey, M.A.; Naud, D.L.; Parrish, D. Synthesis of an Energetic Nitrate Ester. *Angew. Chem. Int. Ed.* **2008**, *47*: 8307-8309.
[10] Fuqiang, B.; Junliang, Y.; Bozhou, W.; Fan, X.-Z.; Ge, Z.-X.; Xu, Ch.; Liu, Q.; Kang, B. Synthesis, Crystal Structure and Properties of 2,3-Bis(Hydroxymethyl)-2,3-dinitro-1,4-butanedioltetranitrate. (in Chinese) *Chin. J. Org. Chem.* **2011**, *31*(11): 1893-1900.
[11] Sizov, V.A.; Pleshakov, D.V.; Asachenko, A.F.; Asachenko, A.F.; Topchiy, M.A.; Nechaev, M.S. Synthesis and Study of the Thermal and Ballistic Properties of SMX. *Cent. Eur. J. Energ. Mater.* **2018**, *15*(1): 30-46.
[12] Reese, D.A.; Son, S.F.; Groven, L.J. Composite Propellant based on a New Nitrate Ester. *Propellants Explos. Pyrotech.* **2014**, *39*(5): 684-688.
[13] Bin, H.; Jinxuan, H.; Xiao-ting, R.; Yilin, C. Synthesis, Crystal Morphology Control of SEM and its Compatibility of HTPB Propellant. (in Chinese) *Chin. J. Energ. Mater.* **2017**, *25*(4): 348-352.
[14] Yang, S.; Qu, J. Computing Thermomechanical Properties of Crosslinked Epoxy by Molecular Dynamic Simulations. *Polymer* **2012**, *53*(21): 4806-4817.
[15] Zhu, W.; Liu, D.M.; Xiao, J.J.; Zhao, X.-B.; Zheng, J.; Zhao, F.; Xiao, H.-M. Molecular Dynamics Study on Sensitivity Criterion, Thermal Expansion and Mechanical Properties of Multi-component High Energy Systems. (in Chinese) *Chin. J. Energ. Mater.* **2014**, *22*(5): 582-587.
[16] Ma, S.; Li, Y.; Li, Y.; Luo, Y. Research on Structures, Mechanical Properties, and Mechanical Responses of TKX-50 and TKX-50 based PBX with Molecular Dynamics. *J. Mol. Model.* **2016**, *22*(2), article 43: 1-11.
[17] Li, M.; Zhao, F.Q.; Xu, S.Y.; Gao, H.X.; Yi, Y.H.; Pei, Q.; Tan, Y.; Li, N.; Li, X. Comparison of Three Kinds of Energy Calculation Programs in Formulation Design of Solid Propellants. (in Chinese) *Chin. J. Energ. Mater.* **2013**, *36*(3): 73-77.
[18] *Material Studio 8.0.* Acceryls Inc., San Diego, **2014**.
[19] Ma, X.; Zhao, F.; Ji, G.; Zhu, W.; Xiao, J.; Xiao, H. Computational Study of Structure and Performance of Four Constituents HMX-based Composite Material. *J. Mol. Struct.: THEOCHEM* **2008**, *851*(1-3): 22-29.

[20] Lu, Y.-y.; Shu, Y.-j.; Liu, N.; Shu, Y.; Wang, K.; Wu, Z.-k.; Wang, X.-ch.; Ding, X.-y. Theoretical Simulations on the Glass Transition Temperatures and Mechanical Properties of Modified Glycidyl Azide Polymer. *Comput. Mater. Sci.* **2017**, *139*: 132-139.
[21] Ewald, P.P. Die Berechnung optischer und elektrostatischer Gitterpotentiale. *Ann. Phys.* **1921**, *369*(3): 253-287.
[22] Karasawa, N.; Goddard III, W.A. Acceleration of Convergence for Lattice Sums. *J. Phys. Chem.* **1989**, *93*(21): 7320-7327.
[23] Andersen, H.C. Molecular Dynamics Simulations at Constant Pressure and/or Temperature. *J. Chem. Phys.* **1980**, *72*(4): 2384-2393.
[24] Berendsen, H.J.C.; Postma, J.P.M.; van Gunsteren, W.F.; DiNola, A.D.; Haak, J.R. Molecular Dynamics with Coupling to an External Bath. *J. Chem. Phys.* **1984**, *81*(8): 3684-3690.
[25] Verlet, L. Computer "Experiments" on Classical Fluids. I. Thermodynamical Properties of Lennard-Jones Molecules. *Phys. Rev.* **1967**, *159*(1): 98-103.
[26] Qian, W.; Shu, Y.; Li, H.; Ma, Q. The Effect of HNS on the Reinforcement of TNT Crystal: a Molecular Simulation Study. *J. Mol. Model.* **2014**, *20*(10), article 2461: 1-7.
[27] Weiner, J.H. *Statistical Mechanics of Elasticity.* Courier Corporation, **2012**; ISBN 9780486161235.
[28] Xu, X.J.; Xiao, H.M.; Xiao, J.J.; Wei Zhu, W.; Huang, H.; Li, J.-S. Molecular Dynamics Simulations for Pure ε-CL-20 and ε-CL-20-based PBXs. *J. Phys. Chem. B* **2006**, *110*(14): 7203-7207.
[29] Watt, J.P.; Davies, G.F.; O'Connell, R.J. The Elastic Properties of Composite Materials. *Rev. Geophys.* **1976**, *14*(4): 541-563.
[30] Pei, J.-F.; Zhao, F.-Q.; Song, X.-D.; Xu, S.-Y.; Yao, E.-G.; Li, M. Calculation and Analysis on Energy Characteristics of High Energy Propellants Based on BAMO/AMMO Copolymers. (in Chinese) *Chin. J. Energ. Mater.* **2015**, *23*(1): 37-42.
[31] Liu, Q.L.; Huang, Y. Transport Behavior of Oxygen and Nitrogen through Organasilicon-Containing Polystyrenes by Molecular Simulation. *J. Phys. Chem. B* **2006**, *110*(35): 17375-17382.
[32] Haesslin, H.W. Dimethylsiloxane-ethylene Oxide Block Copolymers, 2. Preliminary Results on Dilute Solution Properties. *Makromol. Chem.* **1985**, *186*(2): 357-366.
[33] Yu, Z.-F.; Fu, X.-L.; Yu, H.-J.; Qin, G.-M.; Tan, H.-M.; Cui, G.-L. Mesoscopic Molecular Simulation of Migration of NG and BTTN in Polyurethane. (in Chinese) *Chin. J. Energ. Mater.* **2015**, *23*(9): 858-864.

Received: October 6, 2019
Revised: March 19, 2021
First published online: March 30, 2021